Available online at www.sciencedirect.com
SCIENCE DIRECT®
Applied Acoustics 66 (2005) 691–708
applied acoustics
www.elsevier.com/locate/apacoust

Hybrid passive/active absorbers for flow ducts

Marie-Annick Galland *, Benoit Mazeaud, Nadine Sellen

Ecole Centrale de Lyon, Centre Acoustique du LMFA, UMR CNRS 5509, 69134 ECULLY Cedex, France

Received 12 August 2003; received in revised form 22 March 2004; accepted 14 September 2004
Available online 9 December 2004

Abstract

A new type of acoustic liner developed for broadband noise reduction in flow ducts is considered in this paper. It combines passive absorbent properties of a porous layer and active control at its rear face. The complete design procedure of this hybrid passive/active liner is developed here. The passive part is first considered with the determination of a suitable porous material and the cut-off frequency separating the active low frequency regime from the passive high frequency one. The control system is then presented: a digital adaptive feedback control is performed independently cell by cell, allowing an easy subsequent increase of the liner surface. The entire optimization process has been successfully applied to a laboratory flow duct: both predictions and measurements show the interest of the hybrid liner to reduce the noise radiation.

Keywords: Active noise control; Sound absorber; Intelligent materials

1. Introduction

In recent years, noise has become a crucial factor in the design of vehicles, especially in the automotive and aircraft industries. Many research programs have been carried out in order to design efficient noise reduction technologies. Conclusions

* Corresponding author. Tel.: +33 4 72 18 60 13; fax: +33 4 72 18 91 43.
E-mail address: marie-annick.galland@ec-lyon.fr (M.-A. Galland).

0003-682X/$ - see front matter © 2004 Elsevier Ltd. All rights reserved.
doi:10.1016/j.apacoust.2004.09.007

often suggested that combined solutions are the most suited to cover the entire frequency range of unwanted noise. Indeed, passive structures are suited to the reduction of the high frequency contributions of noise and vibrations, while active control technologies appear to be the only way to attenuate the low frequency components. We have developed over the last 10 years a concept of active absorber (see Fig. 1(b)), which combines passive absorption and active control [1]. Olson and May [2] first suggested to perform a pressure reduction at the rear face of a porous layer in order to enhance absorption at low frequencies. Experimental investigations were carried out by Guicking and Karcher [3] and Mechel [4] proposed a similar hybrid system to yield an optimum impedance. Our team has developed and tested such active absorbers for more complex situations such as coupled vibro-acoustic cavities [5] or flow ducts [6]. Substantial and global noise reductions have been obtained for low frequencies with these active absorbers. Our purpose here is to show how such systems, if optimized, are able to deal with both low and high frequency contributions.

Generally, a global noise reduction problem (i.e., a total energy or radiated power reduction) can be formulated in terms of a targeted optimal impedance which has to be achieved on the physical boundaries of the system. In this article, the case of radiation by flow ducts is examined. Tester [7] demonstrated that in the case of a semi-infinite duct with one treated wall, the optimal resistance and the optimal reactance are frequency-dependent, that is to say weak at low frequencies and increasing in absolute value, the targeted reactance always remaining negative. Purely passive materials are unable to reproduce both impedance curves, since bulk materials are inefficient at low frequencies, and resonators or classical liners such as resistive sheets backed by honeycomb structures attenuate only a very limited bandwidth. In the same way, the surface reactance achieved by a purely active absorber is generally close to zero in order to enhance absorption at low frequencies, but this condition becomes inadequate in the higher range of frequencies. Nevertheless, the concept of an active absorber allows us to imagine more extended operating conditions, where active control should be on only at low frequencies. Simultaneously at higher frequencies, the active control is off and the negative reactance is obtained by opti-

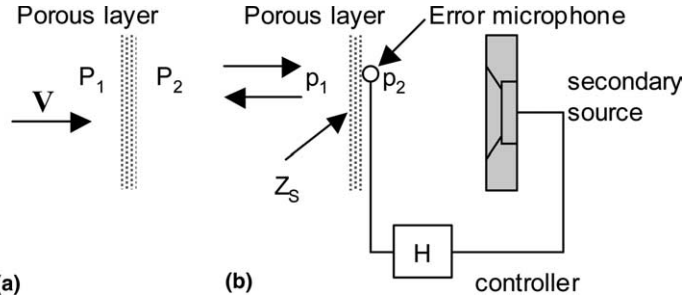

Fig. 1. Hybrid passive/active absorption principle. (a) Low frequency approximation: resistivity. (b) The hybrid passive/active absorber.

mal adjustment of the air gap at the rear face of the porous layer, as for classical liners. The concept of the hybrid absorbent cell is thus introduced, referring to this double operation.

The complete design and optimization of such an absorber is complex. Obviously, it depends on the environment and on the frequency bandwidth of the primary noise. It can be broken down into five steps:

- Determination of the optimal impedance corresponding to the specific environment.
- Design of the passive part: the optimization process is based on the description of the acoustic propagation inside a porous medium. This stage should provide a compromise between a good noise reduction and an achievable hybrid absorber. The cut-off frequency separating the active from the passive operation is also defined at this step.
- Design of the active part: it implies actuator optimization, and controller design.
- Realization of a prototype of the hybrid absorber and validation in a standing wave tube for a single cell.
- Tests in the targeted application with a larger treated area (multi-cell hybrid absorber) and comparison with predictions.

As an example, we present in this paper the complete design process of a hybrid absorber applied to a laboratory set-up, the ECL flow duct called MATISSE. Its simple geometry (in particular, the anechoic termination) allows the determination of a precise modelling of the system. After recalling in a brief section the basic principle of an active absorber, we detail the entire aforementioned process.

2. Basic principle of the active absorber

The basic principle of the active liner has been presented and validated in previous studies (see [1] for instance). It can be summarized as follows: at low frequencies, viscous forces in a porous material predominate over inertial ones and the acoustic behaviour is mainly described by the flow resistivity σ of the material defined by

$$\sigma = \frac{P_1 - P_2}{eV}, \tag{1}$$

where $\Delta P = P_1 - P_2$ is the steady pressure drop across a porous layer of thickness e induced by a steady air flow V.

This static behaviour can also be seen as a limit for the low frequency acoustic behaviour. For a plane wave impinging on a porous sample under normal incidence as shown in Fig. 1(a), it follows that

$$\sigma = \frac{p_1 - p_2}{ev}, \tag{2}$$

where p_1, p_2, and v now represent acoustic quantities.

If the pressure vanishes at the back face, i.e., $p_2 = 0$, the layer input impedance Z_S becomes the flow resistance of the material sample σe. Total absorption is obtained under normal incidence when this impedance matches the characteristic impedance of air, $Z_o = \rho_o C_o$, where ρ_o is the air density and C_o the sound velocity. This property is used when designing passive "$\lambda/4$ absorbers". In this case, the material is placed at a distance equal to a quarter of a wavelength from the rigid wall, in order to reproduce this boundary condition. However, such a technique raises two major problems:

- The required air gap for a low frequency becomes very large (e.g., $\lambda/4 = 0.17$ m in air at 500 Hz).
- The system is only effective in narrow frequency bands, especially for low frequencies.

Active control techniques appear to be particularly efficient in avoiding these drawbacks: the air gap can be replaced by an active control loop which minimizes the pressure (Fig. 1(b)). The secondary source generates a pressure wave, which cancels the primary one by destructive interference at the microphone location, just behind the porous layer. Hence, broadband excitations can be controlled with a reduced absorbent thickness. This method also offers the advantage of separating the control system from a hostile environment (air flow or hot stream for instance).

Different prototypes have been developed in collaboration with METRAVIB [6] in the context of EC projects concerning the noise reduction of aircraft engines. Active absorbers have been studied with the long-term aim of using them as nacelle treatment for the inlet. Numerous and tight constraints such as mechanical constraints, available volume, rapid flow and drainage constraints, led us to adapt the previously developed active absorber. The use of a piezoelectric actuator as secondary source and wire meshes as porous material allowed us to design thin active liners (thickness <0.03 m), see Fig. 2. Their surface impedance is almost real, constant up to 2500 Hz, and approximately equal to the resistance of the cloth. Indeed, for highly resistive materials such as wire meshes, the low frequency behaviour described before

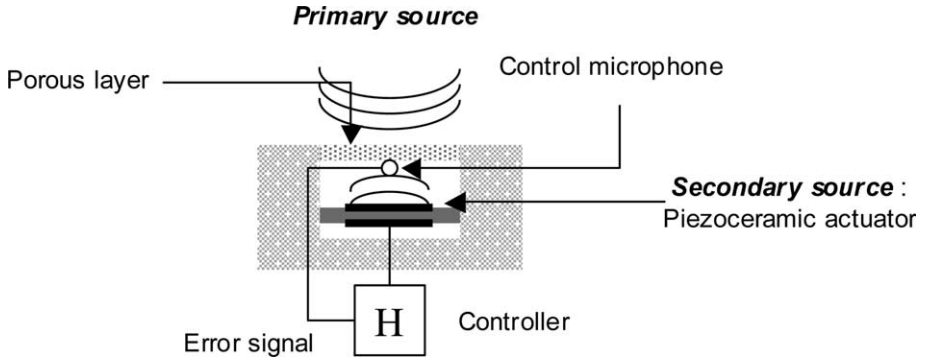

Fig. 2. One-cell hybrid absorber.

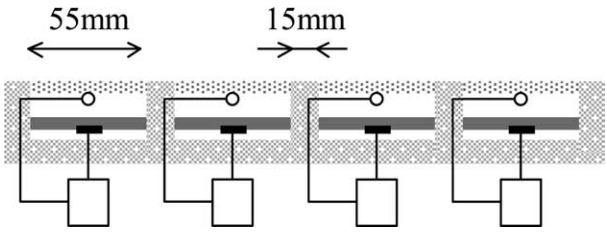

Fig. 3. Extension of the liner surface.

is observed throughout a large frequency range. The transverse size of the cell is determined by the bandwidth of interest. In order to ensure a homogeneous pressure field over the cross-section up to 2500 Hz, the cell is a 55-mm wide square (Fig. 2). Larger active surfaces have been subsequently obtained by juxtaposing cells (Fig. 3). A first series of tests confirmed the ability of active absorbers to achieve noise reduction in flow ducts. We now present new developments, which have been carried out in order to improve the system and its design process, and better to quantify its efficiency.

3. Determination of the optimal impedance

The first stage of the design process is the calculation of the optimal impedance, defined as the wall impedance which minimizes the noise radiated by the flow duct, in the case of the MATISSE ECL facility considered here. Accordingly, this set-up has been modelled in order to calculate the acoustic field obtained with a given wall impedance of finite length and to further deduce the characteristics of the best treatment.

Fig. 4 shows a sketch of the MATISSE flow duct used for further simulations. Calculations are carried out under the following assumptions:

- The duct consists of a square cross-sectional tube of transversal dimensions 0.066×0.066 m^2.
- The MATISSE facility termination is anechoic, i.e., no reflected acoustic waves are generated at the downstream outlet.
- The acoustic treatment characterised by its finite impedance value is applied on the upper wall of the MATISSE flow duct over 0.22 m (i.e., the length of four hybrid cell prototypes). In the following studies, the absorbing wall is assumed to be locally reacting.

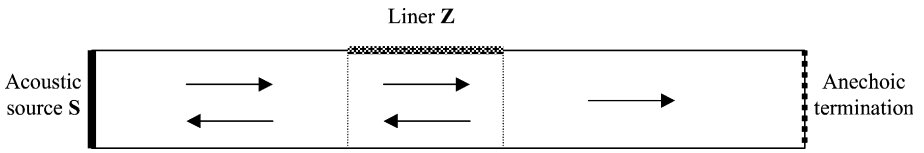

Fig. 4. MATISSE flow duct simplified representation, calculation configuration.

- The flow velocities considered in the simulations do not exceed 50 m/s and the analysis covers the frequency range 500–2500 Hz, corresponding to the plane wave limit for the MATISSE duct.

The multimodal expansion method proposed by Roure [8] has been extended to account for a uniform flow (the detailed modelling is described by Sellen et al. [9]). The source (S) is a uniform velocity piston covering the entire inlet duct cross-section, and only incident waves are considered in the last part of the tube downstream the absorbing wall region. Inside the treated area, the eigenfunctions are determined via a finite-difference approach. The transmission loss, defined as the ratio of the incident power to the transmitted one, is the energetic indicator selected to evaluate the liner performance. It is calculated in the impedance plane for both given frequency and flow velocity. The optimal resistance and reactance are obtained from the location of the maximal value of transmission loss. Fig. 5 shows the real and imaginary part values of the optimal impedance versus frequency, plotted for three different flow velocities: 0, 20 and 50 m/s. It should be noted that the two curves are frequency dependent, increasing in absolute value with frequency. Moreover, the targeted reactance is always negative. Finally, the influence of flow velocity does not seem to be very important in this range. This behaviour conforms to the results obtained by Cremer [10] (no flow case) and those obtained later by Tes-

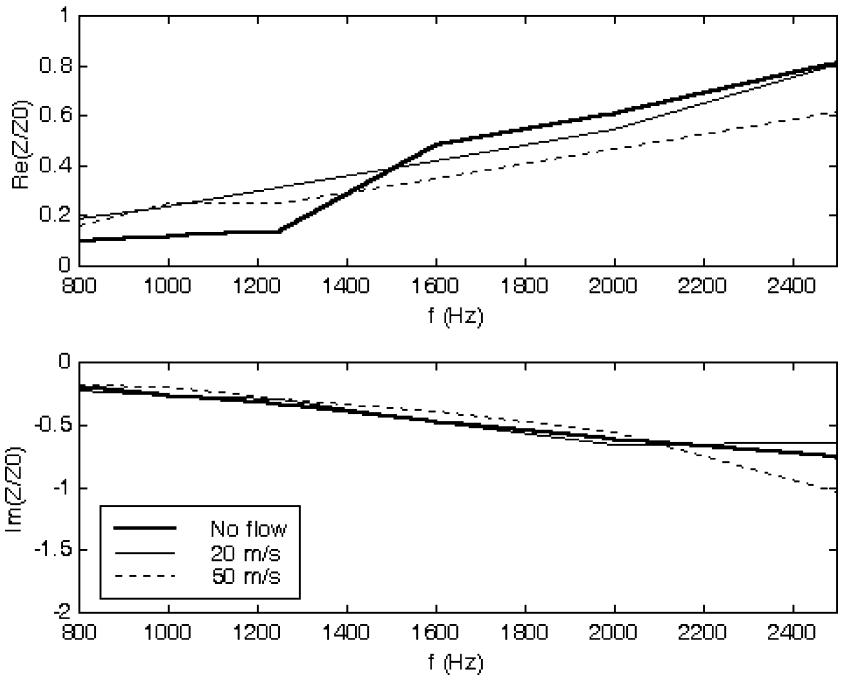

Fig. 5. Real and imaginary part values of the optimal impedance versus frequency for different flow velocities.

ter [7] (with a uniform flow), although in their calculations the impedance boundary condition was applied to the entire wall. Obviously, a purely active absorber using a wire mesh as a passive layer cannot provide these impedance values and a "better" porous material must be found, by developing an appropriate modelling of the active absorber. The porous layer behaviour is thus described by using the fluid-equivalent model by Johnson and Allard [11]. The pressure cancellation obtained by active control at the error microphone is supposed to be perfect and an impedance value of zero is set at the rear face of the porous layer. Transporting the zero value through the material allows the calculation of the surface impedance presented by the liner. The following simplified expression is obtained in the case of low frequencies by the 1st order approximation:

$$Z_S = \sigma e + je\left[\frac{\alpha_\infty \rho_o}{\varphi}\left(1+\frac{1}{4s^2}\right) - \frac{\sigma^2 e^2 \varphi}{3P_o}\right]2\pi f. \tag{3}$$

In this expression, we introduce the main parameters of the porous material, i.e., thickness e, resistivity σ, porosity φ, tortuosity α_∞ and viscous shape factor s, the air characteristics – pressure P_o and density ρ_o – and the wave frequency f. Thus, at very low frequencies, the front face impedance is almost purely real and equal to the flow resistance of the material sample σe (see Eq. (2)). The frequency dependence of the reactance is linear and the slope is negative only if

$$\sigma^2 e^2 \geqslant \frac{3P_o \alpha_\infty \rho_o}{\varphi^2}\left(1+\frac{1}{4s^2}\right).$$

The previous condition leads to

$$\sigma e \geqslant \sqrt{\frac{15}{4}P_o \rho_o} \approx 1.64\ \rho_o C_o$$

when φ, α_∞ and s all reach the value of 1.

In other words, one cannot find a porous material leading to a negative reactance and a sufficiently weak resistance at its front face when pressure cancellation is achieved at its rear face. A purely active absorber is thus not suited for the reproduction of the optimal impedance shown in Fig. 5. A hybrid absorber can therefore be imagined, using active control for low frequencies and the actuator plate as a rigid wall for higher frequencies, this last device providing the negative reactance. The hybrid operation is illustrated in Fig. 6. The surface impedance provided by the hybrid absorber in passive mode can be estimated by transporting the rigid wall's infinite impedance to the rear face of the porous layer through the air gap, and then through the material. Many configurations have been tested in order to determine the best compromise, i.e., the device which is able to achieve the best noise reduction throughout the entire frequency range of interest. The intrinsic material characteristics, its thickness, the air gap depth d and the cut-off frequency f_c separating the active from the passive operation are the main parameters in this problem, see Fig. 6. Finally, resistive sheets seem to be the materials best suited to our application. The surface impedance obtained in this case can be approximated by:

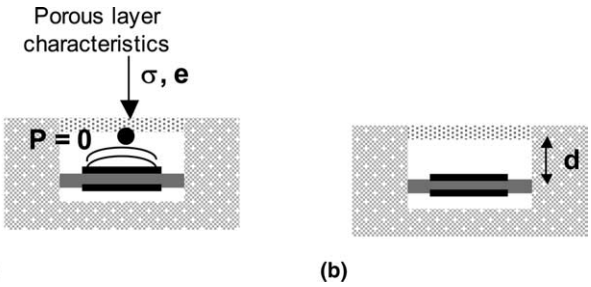

Fig. 6. Hybrid operation for the sound absorbing cell. (a) Low frequency: pressure release, from 500 Hz to f_c. (b) High frequency: air cavity, from f_c to 2500 Hz.

$$\begin{aligned} Z_S &= \sigma e \text{ in active mode} \\ Z_S &= \sigma e - j\rho_o C_o \cot(2\pi f d/C_o) \text{ in passive mode.} \end{aligned} \tag{4}$$

The best compromise is obtained for a resistive layer whose resistance is close to $0.3\rho_o C_o$, which is approximately the mean value of the targeted optimal resistance. Fig. 7 represents the transmission loss in the frequency range [500 Hz, 2500 Hz] with a step of 250 Hz, obtained for different boundary conditions applied at its rear face, without and with flow (50 m/s). The active mode corresponds to the pressure cancellation ($P = 0$) and the passive mode performance is plotted for different depths of the rear cavity. It results that the best compromise, which combines high noise reduction and compactness of the hybrid liner, is obtained for an air gap depth of 0.02 m and for a cut-off frequency of 1800 Hz. The practical implementation is achieved through an existing wire mesh whose resistance is close to the theoretical one.

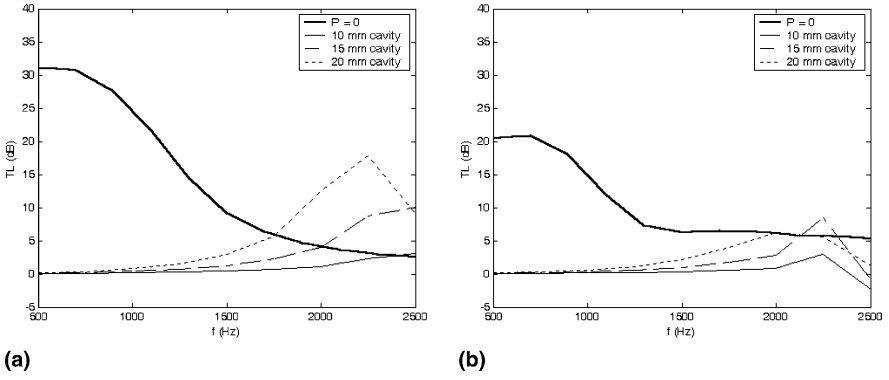

Fig. 7. Transmission loss predicted for different cell configurations and boundary conditions. (a) No flow. (b) Flow velocity 50 m/s.

4. Design of the active control system

For industrial applications, the absorbent surface has to be increased, and it is therefore necessary to consider hybrid cells in very large numbers. Experiments were first carried out using a four-cell system outfitted with a digital feedforward controller [12]. Significant noise reductions were obtained in the frequency range 1000–2100 Hz.

However, with a Multiple Input Multiple Output (MIMO) feedforward system, memory and calculation costs significantly increase with the number of channels. Moreover, in many applications such as turbojet inlet lining, an upstream reference noise input may be insufficiently correlated with the sound to be cancelled, to achieve high noise reduction. Thus, feedback control is preferable. Analogue feedback controllers were also tested [6] but with poor results because their design is very complex for resonant actuators such as the piezoelectric one used here, and it depends strongly on the electro-acoustic response in each cell. As discrepancies always occur in the manufacturing of the cells, an individual control filter has to be designed for each of them. Therefore, only independent active cells with adaptive digital controllers can be considered in order to extend the treated area for industrial applications. We present here a system which allows a digital adaptive control cell by cell. The Single Input Single Output (SISO) version of the algorithm consists in removing the feedback contribution, thus leading to a feedforward behaviour. The classical FXLMS algorithm can then be used with a reconstructed reference signal, which corresponds to the primary noise, if the feedback is well modelled. This architecture was first proposed by Elliott and is called Internal Model Control [13]. The extension to MIMO systems proposed by Kuo and Morgan [14] consists in removing all secondary contributions and furthermore is too complex for a large number of channels, as previously described for a feedforward system. We have developed and tested a simplified version, in which only the self (and main) feedback produced by each cell is removed. The main conclusion of the theoretical study is that the physical coupling occurring between active cells can produce a global unstable behaviour even if the optimal filter is realized in each cell. An adaptive band-pass filter is therefore used to prevent instabilities [15]. The control algorithm is represented in Fig. 8 for a two-cell system. The transfer function of the control filter is $W_1(z)$ for the first cell and $W_2(z)$ for the second one. The total error signals at the two microphones, e_1 and e_2, deployed in cell 1 and cell 2, respectively, are the sum of the primary signals d_1 and d_2 and the secondary signals coming from each secondary source via the self secondary path S_{11} or S_{22} and via the crossed path S_{12} or S_{21}. The controller outputs y_1 and y_2, from which the self-contribution has been removed thanks to an off-line estimation of the corresponding transfer, are used to build the references x_1 and x_2, which consequently differ in this algorithm from the primary signals. Stability is ensured via a band-pass filtering of the reference signals.

We present here some simulation results concerning the two-cell system, in order to examine if this algorithm is adapted to the specific hybrid functioning. The primary noise consists of two tones at 1500 and 2000 Hz emerging from a broadband random noise. This signal is representative of experimental conditions

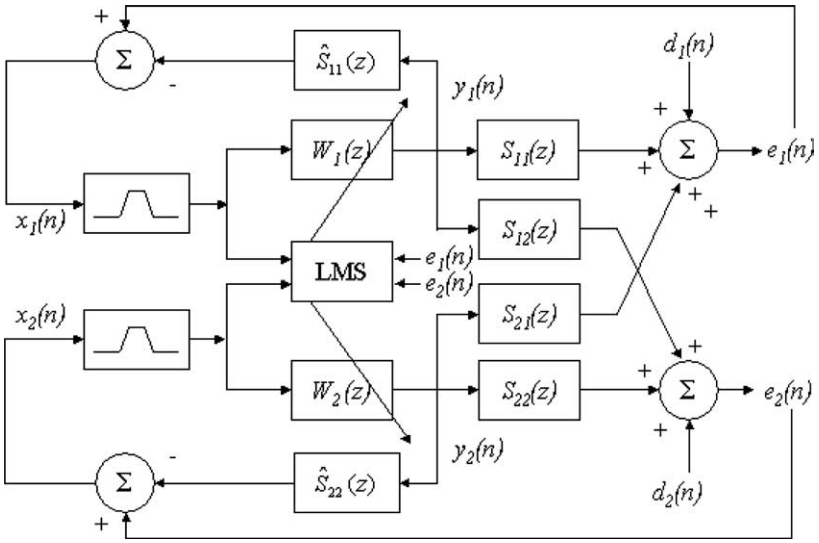

Fig. 8. The IMC-MDFXLMS architecture.

encountered in a flow duct. As shown in the previous section, only the first tone must be reduced at the control microphones. A zero-velocity (rigid wall) boundary condition must be ensured at the actuators for the second tone because the

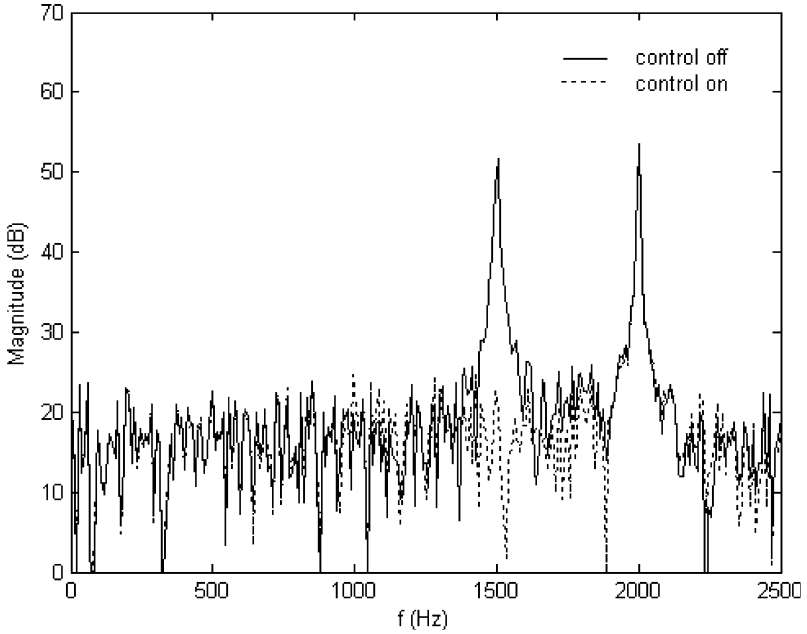

Fig. 9. Pressure spectrum at one microphone.

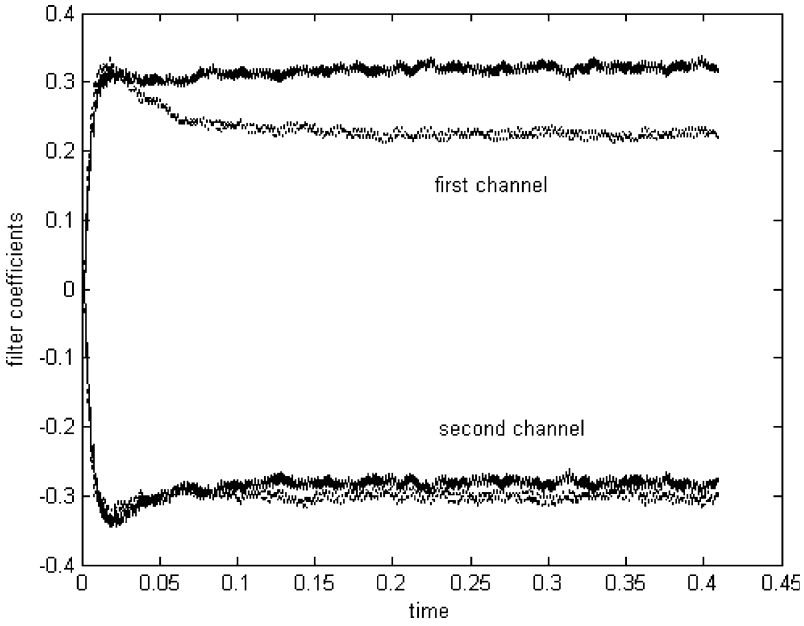

Fig. 10. Time evolution of the filter coefficients.

frequency limit for active control has been set to 1800 Hz. The noise spectrum at one control microphone is plotted in Fig. 9: the 1500 Hz contribution is strongly reduced, while the level of the 2000 Hz tone is unchanged. The same behaviour is observed at the second microphone. The time evolution of the filter coefficients is represented in Fig. 10 for each channel of the control system. Convergence is obtained very rapidly with this algorithm even with a strong background noise contribution as is the case here. In this example, the sampling frequency is 10 kHz, the band-pass filter is a recursive digital filter of second order and only two taps are sufficient for each control filter. Thus, the algorithm seems able to work as required for the hybrid cell in a flow duct.

5. The MATISSE experimental test bench

The MATISSE experimental flow duct, represented in Fig. 11, consists in a square cross-sectional duct (0.066×0.066 m^2) whose axial length is approximately 3.20 m. A quiet flow generator system induces a silent flow of maximal velocity 50 m/s inside the tube. The anechoic downstream termination is achieved thanks to an exponential outlet. The test section has been designed and manufactured in order to evaluate the efficiency of conventional passive treatments as well as of the hybrid prototypes. The hybrid liners are applied on the upper wall of the test

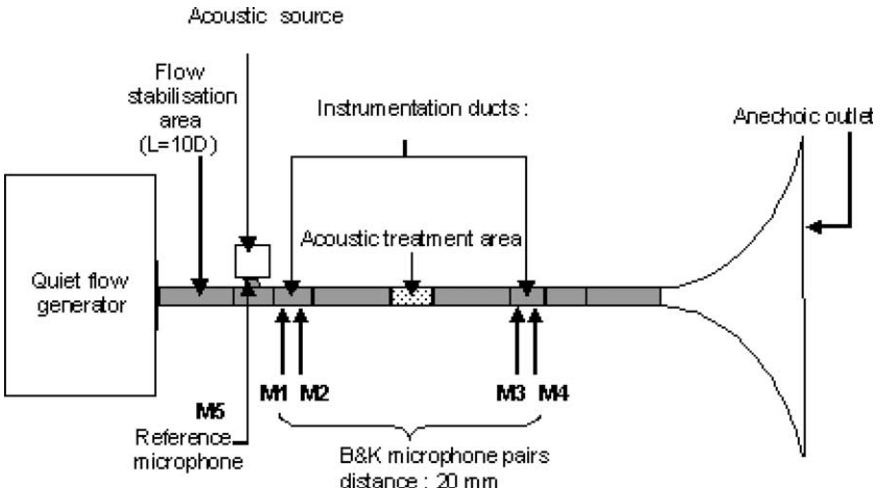

Fig. 11. The MATISSE flow duct.

section over a distance of 0.22 m. Four flush-mounted microphones (B&K 1/4'') located upstream (M1–M2) and downstream (M3–M4) the test region measure the differential pressure to characterise the acoustic performance of the MATISSE flow duct with and without the tested liners. The total length of the instrumentation duct, i.e., from M1 to M4, is 1.26 m. Each microphone pair M1–M2 and M3–M4 allows one to separate incident from reflected waves. Reliability of the exponential termination can thus be verified by evaluating the incident to reflected component ratio for the entirely rigid walled duct. Furthermore, the transmission loss parameter can be estimated for each acoustic treatment inserted in the test section. A fifth microphone M5 has been placed close to the primary source in order to record the sound levels generated.

The frequency response functions between each microphone (M1–M5) and the primary source are recorded using IDEAS® software. Reflection coefficient and transmission loss values are then computed using MATLAB®. As in the theoretical study of preceding sections, the transmission loss measurements on the MATISSE facility are carried out up to 2500 Hz, i.e., in the plane wave frequency range of the duct.

The hybrid absorber prototype, represented in Fig. 12(a), was manufactured using the different specifications established through previous passive and active optimization stages. Particular attention was paid to the design of the secondary source, which was done in collaboration with METRAVIB. The piezoelectric thin-layer technology was finally selected because it provides a good compromise between thickness and acoustic efficiency. The basic principle consists in exciting an aluminum plate in a flexural deformation mode. The hybrid liner tested on the MATISSE flow duct is composed of four hybrid cells, see Fig. 12(b).

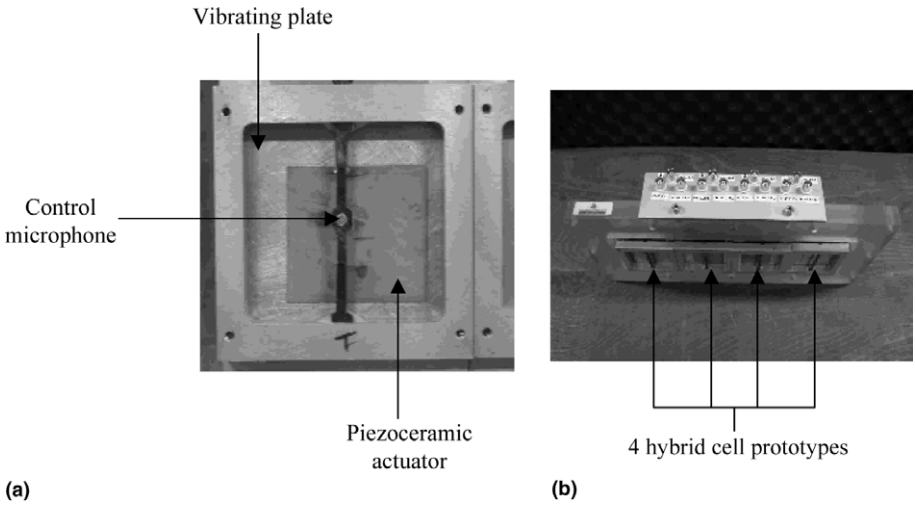

Fig. 12. The hybrid liner prototype. (a) One-cell prototype. (b) Four-cell prototype.

6. Experimental results

In order to validate the theoretical results, we first experimented in a standing wave tube with a wire mesh having a resistance close to $0.3\rho_o C_o$. The surface impedance is measured for the active or passive operation with a broadband excitation in both cases. Active control is performed by a feedforward control algorithm, the reference signal being taken at the primary source. The wire mesh is located at 0.02 m from the actuator plate, as suggested by the theoretical study. Comparisons are presented in Fig. 13(a) and (b) with the theoretical optimal curves. As expected, the effect of the active control is to achieve reactance values close to zero. This effect is

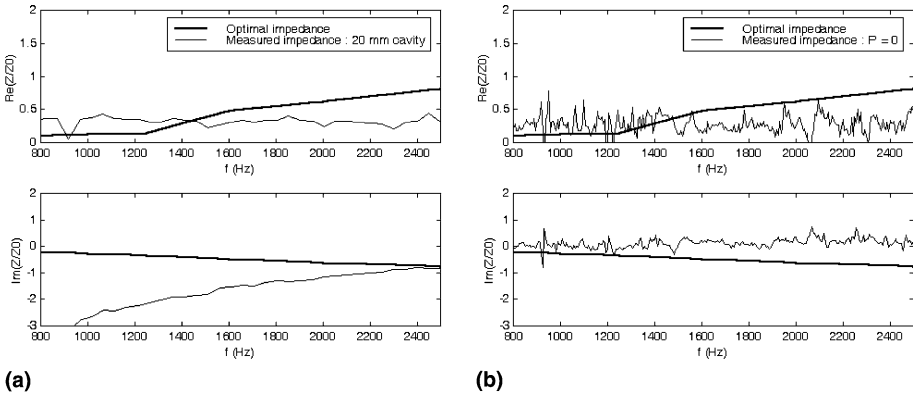

Fig. 13. Comparison between measured and optimal impedance, standing wave tube measurements. (a) Passive operation. (b) Active operation.

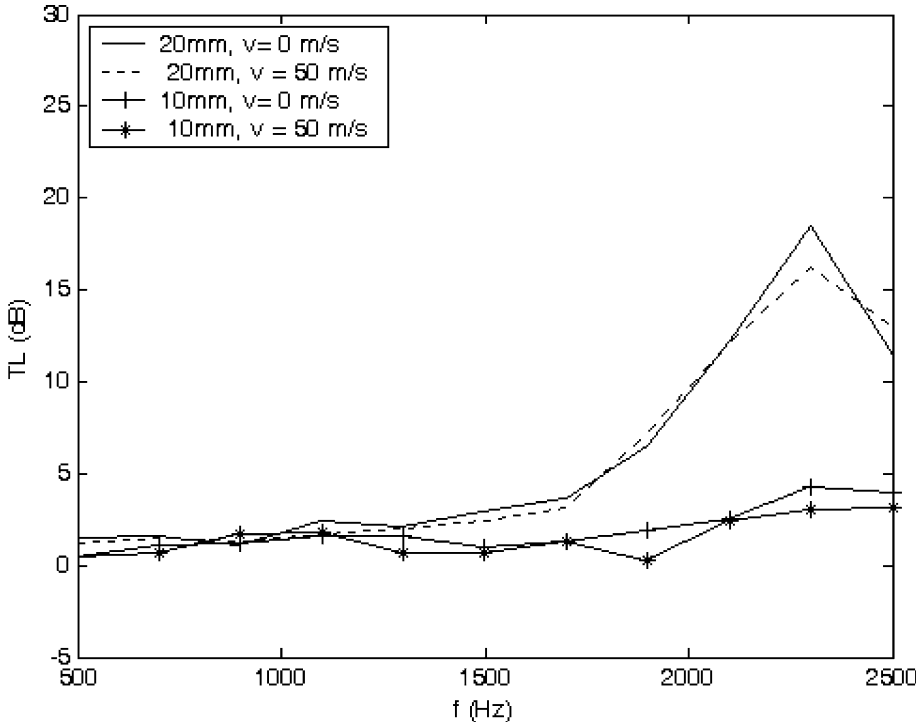

Fig. 14. Transmission loss measured for the four-cell absorber. Passive operation for two distances between actuator and wire mesh and two flow velocities.

positive at low frequencies, where the reactance becomes strongly negative in the passive operation owing to the air gap contribution. At higher frequencies, the optimal reactance must be negative and active control is not well suited. The real hybrid cell is thus able to provide impedance values relatively close to the optimal ones, with a cut-off frequency of 1800 Hz.

The passive behaviour in the MATISSE flow duct has been tested with a four-cell prototype of the hybrid absorber described previously. Two distances between actuator and wire mesh have been tested: 0.01 and 0.02 m. The results are plotted in Fig. 14 for two flow velocities. They are in very good agreement with the predictions shown in Fig. 7, and yet the calculated optimal impedance or transmission loss values have been obtained under the assumption of a locally reacting material. This means that plane waves are supposed to propagate only normally to the mesh surface in the air gap at its rear face. Thus, the grazing incidence encountered in the MATISSE flow duct seems to have a negligible impact on the material behaviour. To conclude, these first experimental results validate both the modelling and measurement processes. A purely passive absorber of reasonable thickness is clearly unable to provide noise reduction at low frequencies.

The efficiency of an active system is strongly related to the transfer function between the secondary source and the error sensor in the real environment. Power, linearity and weak sensibility to the external conditions are some of the required qualities. The frequency response functions between an actuator and its associated error sensor have been measured in the MATISSE duct for different configurations and flow velocities They are plotted in Fig. 15 in magnitude and phase, for a particular active cell either closed by a wire mesh or uncovered. High amplitudes are encountered in the frequency band where active control is required, the plate resonance occurring at about 1100 Hz. Sound pressure levels higher than 130 dB can be achieved at the control microphone in this band. We also observe the positive effect of the resistive sheet, which slightly increases the sound level and reduces the influence of the external environment (the MATISSE duct) appearing as oscillations occurring at regular intervals. The same measurements have been carried out with flow, but it is impossible to measure correctly the acoustic pressure, and thus to control it, if no wire mesh separates the error microphone from the flow. The wire mesh allows the active system to operate satisfactorily. Moreover, measurements show that the response is not very sensitive to the flow velocity in the bandwidth of interest. This property is very interesting for active control applications because it enhances the system's robustness.

The control algorithm was then implemented on a dSPACE-DS1103 controller board equipped with a TI-TMS320F240 floating-point DSP, thanks to MATLAB/Simulink®. Preliminary tests were carried out with two active cells mounted on

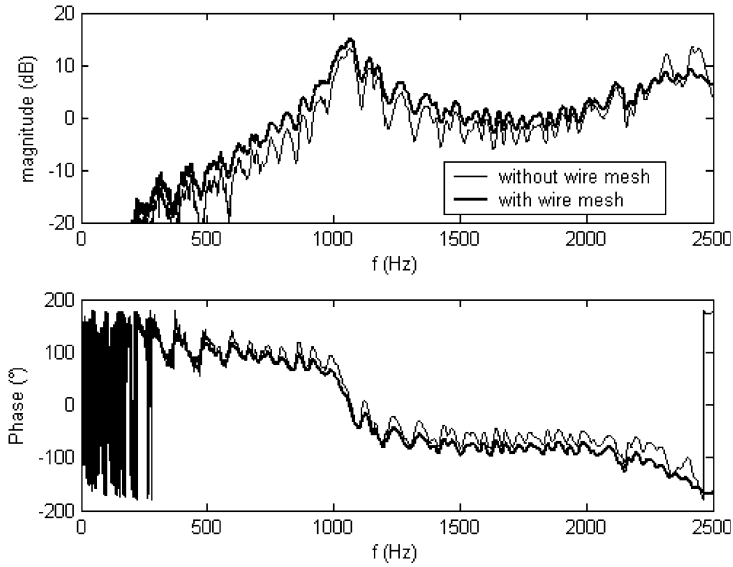

Fig. 15. Measured frequency response functions between actuator and error sensor. No flow case.

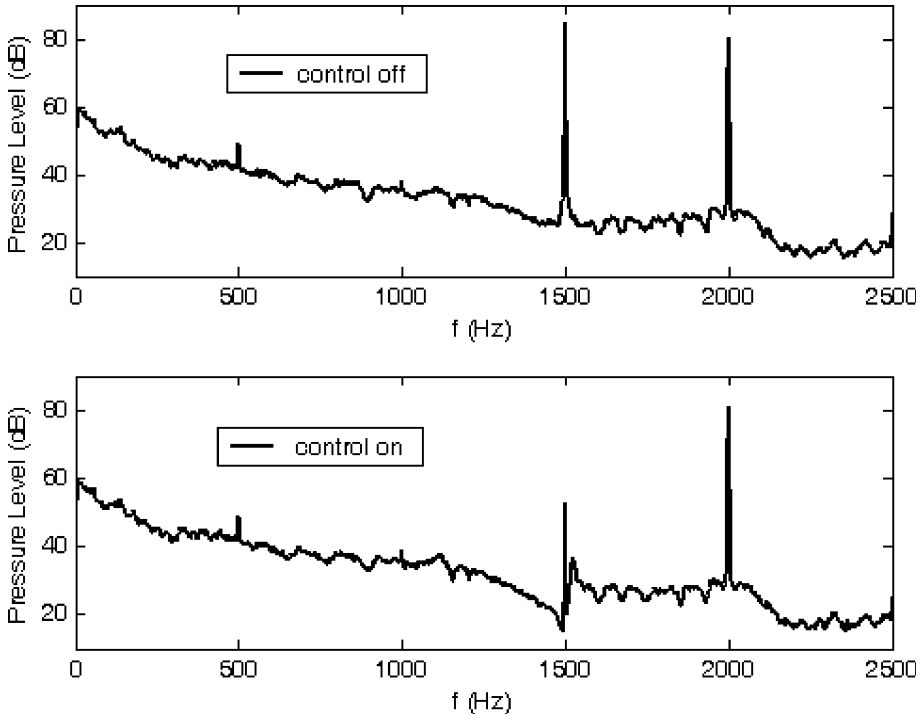

Fig. 16. Pressure spectrum measured at one microphone, without and with control.

the MATISSE duct wall. They demonstrated the satisfactory behaviour of the active system in the same conditions as those described in the simulation part. As an example, the pressure spectrum measured at one error microphone is plotted in Fig. 16 and shows that the two-cell feedback control algorithm is able to deal with a two-tone noise: the lower one is reduced without any disturbing effect on the higher one. The flow velocity in this experiment reaches 20 m/s. If the secondary path between each actuator and its associated control sensor is precisely modelled, convergence of the algorithm is obtained very rapidly; noise reduction is substantial and stability ensured.

The system was later successfully tested with a four-cell prototype in the MATISSE duct with a flow velocity of up to 50 m/s. The transmission loss is plotted in Fig. 17 for two flow velocities. Active control was performed only up to 1700 Hz because there is no interest in such a system for higher frequencies. The greatest noise reduction is obtained at low frequencies and the general behaviour is in very good agreement with the theoretical predictions shown in Fig. 7. Thus, the hybrid absorber behaves as predicted for active or passive functioning. Indeed, combining the two operations allows the design of a thin absorber able to provide a significant transmission loss throughout the entire frequency range.

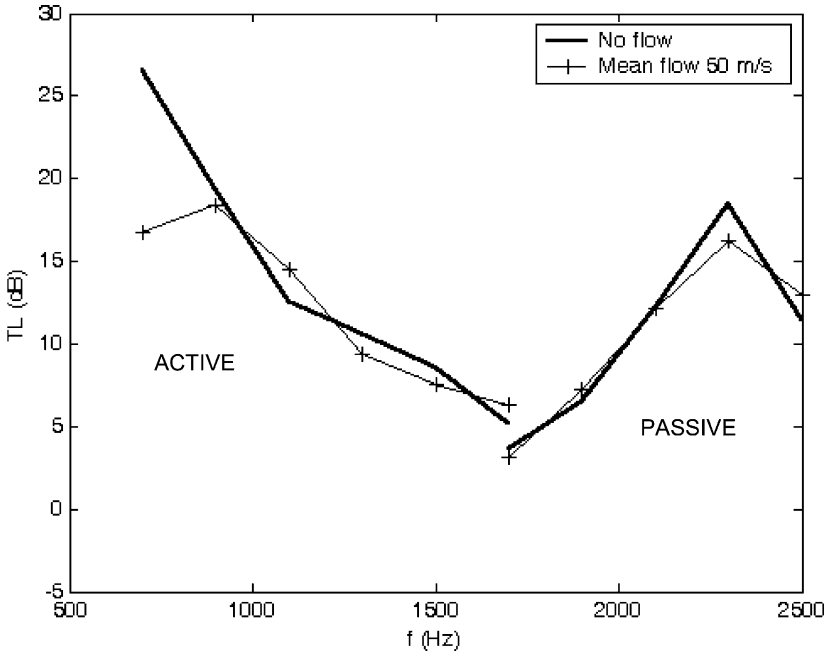

Fig. 17. Transmission loss measured for the four-cell absorber. Passive or active operation for two flow velocities.

7. Conclusion

The complete optimization process of a hybrid absorber has been described in the case of a laboratory flow duct. The optimal impedance is first determined by modelling the set-up, and the best compromise is realized from existing materials. The cut-off frequency which separates active from passive operation and the cavity depth at the rear face of the porous layer are important parameters. This optimal configuration depends on the geometrical conditions, on the absorber size and location, and on the frequency range. For our application the optimal cell is obtained with a resistive sheet located at 0.02 m from the actuator plate. Large absorbent areas can be manufactured because the active boundary condition is achieved independently cell by cell via a new algorithm, allowing digital adaptive feedback control to work without instabilities. Multi-tone noise can be reduced automatically at each cell. The combined passive/active operation allowed us to achieve significant noise reductions, between 8 dB and about 20 dB in our flow duct, for velocities up to 50 m/s with a treated area of 0.22 m by 0.055 m. This optimization process is general and can be reproduced for any complex set-up. Further experiments will be carried out with larger absorbent surfaces and higher flow velocities.

Acknowledgement

This study was supported in part by the EC in the context of the SILENCE(R) project (GRD1-2000-25297).

References

[1] Furstoss M, Thenail D, Galland MA. Surface impedance control for sound absorption: direct and hybrid passive/active strategies. J Sound Vib 1997;203(2):219–36.
[2] Olson HF, May EG. Electronic sound absorber. J Acoust Soc Am 1953;25:1130–6.
[3] Guicking D, Karcher K. Active sound absorber with porous plate. ASME J Vib Acoust, Stress Reliab Des 1984;106:393–6.
[4] Mechel FP. Hybrider Schalldämpfer. Patent No. DE 4027511.
[5] Lacour O, Galland MA, Thenail D. Preliminary experiments on noise reduction in cavities using active impedance changes. J Sound Vib 2000;230(1):69–99.
[6] Galland MA, Souchotte P, Ladner P, Mazoyer T. Experimental investigation of noise reduction in a flow duct through hybrid passive/active liner. In: 7th AIAA/CEAS aeroacoustics conference, Maastricht, The Netherlands; 28–30 May 2001. p. 2001–221..
[7] Tester BJ. The propagation and attenuation of sound in lined ducts containing uniform or ''plug'' flow. J Sound Vib 1973;28(2):151–203.
[8] Roure A. Propagation du son dans des conduits à section variable. Application à la détermination des fréquences propres de certains volumes complexes. In: Euromech 94, L.M.A. Marseille; 12–15 September 1977.
[9] Sellen N, Cuesta M, Galland MA. Passive layer optimization for active absorbers in flow duct applications. In: 9th AIAA/CEAS aeroacoustics conference, Hilton Head, South Carolina. AIAA; 12–14 May 2003. p. 2003–3186.
[10] Cremer L. Theorie des Luftschall-Dampfing im Rechteckkanal mit schluckender Wand und das sich dabei ergebende hochste Dampfungsmass. Acustica 1953;2:249–63.
[11] Allard JF. Propagation of sound in porous media. London: Elsevier Applied Science; 1993.
[12] Galland MA, Sellen N, Hilbrunner O. Noise reduction in a flow duct by active control of wall impedance. In: 8th AIAA/CEAS aeroacoustics conference, Breckenridge, Colorado. AIAA; 17–19 June 2002. p. 2002–498.
[13] Elliott SJ, Sutton TJ, Rafaely B, Johnson M. Design of feedback controllers using a feedforward approach. Active 1995;95:561–72.
[14] Kuo SM, Morgan DR. Active noise control systems. Wiley; 1996.
[15] Hilbrunner O, Mazeaud B, Galland MA. Multi-cell digital feedback control for noise reduction through hybrid absorbers. In: 9th AIAA/CEAS aeroacoustics conference, Hilton Head, South Carolina. AIAA; 12–14 May 2003. p. 2003–3187.